Nanoscale

Interaction studies reveal specific recognition of an anti-inflammatory polyphosphorhydrazone dendrimer by human monocytes

Journal:	*Nanoscale*
Manuscript ID:	NR-ART-06-2015-003884.R1
Article Type:	Paper
Date Submitted by the Author:	22-Jul-2015

Complete List of Authors:	Ledall, Jérémy; INSERM, CNRS, Université de Toulouse, ; CNRS, LCC (Laboratoire de Chimie de Coordination), Fruchon, Séverine; INSERM, CNRS, Université de Toulouse, Centre of Physiopathology of Toulouse-Purpan; CNRS, LCC (Laboratoire de Chimie de Coordination), Garzoni, Matteo; university of applied science of southern switzerland (SUPSI), Mathematical and physical sciences research unit (SMF) Pavan, Giovanni M.; University of Applied Science of Southern Switzerland, Department of Innovative Technologies Caminade, Anne-Marie; CNRS, LCC (Laboratoire de Chimie de Coordination), Turrin, Cedric-Olivier; CNRS, Laboratoire de Chimie de Coordination UPR8241 Blanzat, Muriel; Lab. IMRCP, UMR CNRS 5623, Poupot, Rémy; INSERM, CNRS, Université de Toulouse, Centre of Physiopathology of Toulouse-Purpan

SCHOLARONE™
Manuscripts

Interaction studies reveal specific recognition of an anti-inflammatory polyphosphorhydrazone dendrimer by human monocytes†

Jérémy Ledall,[a,b] Séverine Fruchon,[a,b] Matteo Garzoni,[c] Giovanni M. Pavan,[c] Anne-Marie Caminade,[b] Cédric-Olivier Turrin,*[b] Muriel Blanzat*[d] and Rémy Poupot*[a]

[a] *INSERM, UMR1043, CNRS, U5282, Université de Toulouse, UPS, Center of Physiopathology of Toulouse-Purpan, CHU Purpan, BP 3028, Toulouse F-31300, France*

[b] *CNRS, UPR 8241, Université de Toulouse, UPS, INPT, Laboratoire de Chimie de Coordination, 205 route de Narbonne, BP 44099, Toulouse F-31077, France*

[c] *Department of Innovative Technologies, University of Applied Sciences and Arts of Southern Switzerland, Galleria 2, Manno 6928, Switerland*

[d] *Laboratoire IMRCP, CNRS UMR 5623, Université de Toulouse, UPS, 118 route de Narbonne, Toulouse F-31062, France.*

† Electronic supplementary information (ESI) available.

* Corresponding authors. *E-mail addresses:* cedric-olivier.turrin@lcc-toulouse.fr, blanzat@chimie.ups-tlse.fr, remy.poupot@inserm.fr

Keywords: phosphorous-based dendrimers; human monocytes; immuno-modulation; molecular simulations; binding; nanobiotechnology; membrane interaction.

Table of contents entry: *Specific interaction and internalisation of an AzaBisPhosphonate-capped polyphosphorhydrazone dendrimer leads to the anti-inflammatory activation of human monocytes.*

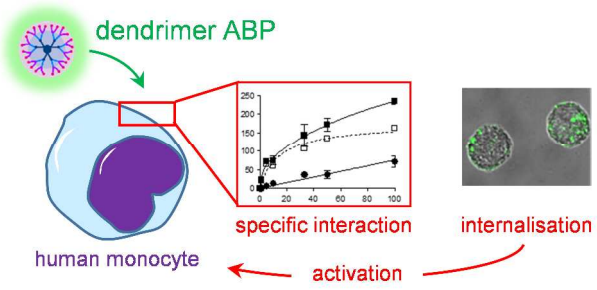

ABSTRACT

Dendrimers are nano-materials with perfectly defined structure and size, and multivalency properties that confer substantial advantages for biomedical applications. Previous work has shown that phosphorous-based polyphosphorhydrazone (PPH) dendrimers capped with azabisphosphonate (ABP) end groups have immuno-modulatory and anti-inflammatory properties leading to efficient therapeutical control of inflammatory diseases in animal models. These properties are mainly prompted through activation of monocytes. Here, we disclose new insights in the molecular mechanisms underlying the anti-inflammatory activation of human monocytes by ABP-capped PPH dendrimers. Following an interdisciplinary approach, we have characterized the physicochemical and biological behavior of the lead ABP dendrimer with model and cell membranes, and compared these experimental set of data to predictive computational modelling studies. The behavior of the ABP dendrimer was compared to the one of an isosteric analog dendrimer capped with twelve azabiscarboxylate (ABC) end groups instead of twelve ABP end groups. The ABC dendrimer displayed no biological activity on human monocytes, therefore it was considered as a negative control. In detail, we show that the ABP dendrimer can bind both non-specifically and specifically to membrane of human monocytes. The specific binding leads to the internalization of the ABP dendrimer by human monocytes. On the contrary, the ABC dendrimer only interacts non-specifically with human monocytes and is not internalized. These data indicate that the bioactive ABP dendrimer is recognized by specific receptor(s) at the surface of human monocytes.

1. Introduction

Dendrimers are non-linear, hyperbranched, and multivalent polymers that have invested the fields of nanobiology and nanomedicine.[1] Indeed, the control of their size and structure during the synthesis affords tuneable isomolecular compounds. Dendrimers are built starting from a central core to which are linked one or several series of radial monomers (the so-called branches). Each monomer is ended by a point of divergence, enabling the dendritic growth of the molecule by addition of the next generation of branches. The synthesis ends with the addition of functional groups at the outermost series of branches. The multivalency of dendrimers is a fundamental property for biomedical applications as polyvalent interactions are ubiquitous in biology.[2] Therefore, it was commonly thought that the chemical composition and the number of the surface groups were the key determinants of the bioactivity of dendrimers. However, six Critical Nanoscale Design Parameters (CNDPs) for dendrimers (size, shape, surface chemistry, flexibility/rigidity, architecture and elemental composition) has been proposed recently.[3] It is worth noting that among the CNDPs, at least three (size, flexibility/rigidity, and architecture) are directly related to the internal dendritic structure. Recently we have demonstrated unambiguously that the dendritic scaffold is not an inert carrier of the surface groups of the molecules as the overall three-dimensional conformation induced by the entire structure (including the core and the branches) is crucial for the efficiency of dendrimer nanodrugs.[4] For example, to increase the ability of the dendrimer to establish multivalent interactions, the number of surface groups is not the unique important variable, but it is essential that the dendrimer can re-orient and gather the surface functionalities to increase the density of active groups. This clearly pertains to the flexibility/rigidity of the internal scaffold, and to the overall conformation that the dendrimer assumes in the solvent. In particular, Poly(PhosphorHydrazone) (PPH)

dendrimers ended with phosphonate groups have the required directional conformation which enables their immuno-modulatory properties toward the human immune system *in vitro*.[5–9] Moreover, the anti-inflammatory properties of a first generation PPH dendrimer functionalized at its surface with twelve azabisphosphonate groups (dendrimer **1**, Fig. 1) have been challenged *in vivo* in animal models of chronic and acute inflammatory diseases. The dendrimer **1** has proven its efficacy in rodent models of both experimental arthritis (chronic disease)[10] and endotoxin-induced uveitis (acute disease).[11] This unique molecule is a promising drug-candidate for the treatment of inflammatory diseases in human[12] as it does not show any general or immunological sub-chronic toxicity in a non-human primate model after repeated intravenous injections.[13] Among human Peripheral Blood Mononuclear Cells (PBMC), we have shown that the dendrimer **1** primarily targets monocytes and activates them toward an anti-inflammatory pathway.[5,6]

Herein, by combining chemistry with computational, physicochemical, and biological studies, we disclose new results related to the understanding of the interactions between the dendrimer **1** and human monocytes *in vitro*. The physicochemical and biological behavior of dendrimer **1** has been compared to those of an isosteric analog bearing twelve azabiscarboxylate groups (dendrimer **2**, Fig. 1) which had been synthesized previously.[14] In a first step, computational analyses has provided the molecular description of the non-specific adsorption of both dendrimers on a phospholipidic bilayer. Then, physicochemical studies have confirmed the computational assessments, showing very weak non-specific interactions of both dendrimers with models of phospholipidic bilayers. In a last step, biological experiments have shown that, contrary to dendrimer **1**, dendrimer **2** is unable to activate human monocytes *in vitro*. On the same track, experimental biochemical studies have indicated that dendrimers **1** and **2** have

different abilities to bind to human monocytes *in vitro*, resulting in the internalization of the former, unlike the latter.

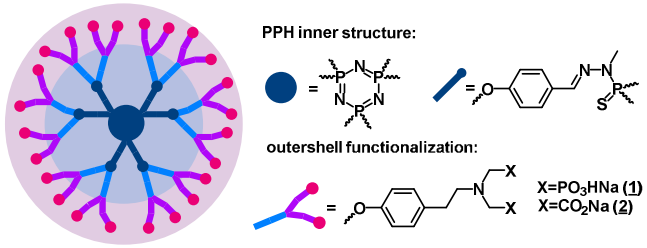

Fig. 1 Structure of dendrimers **1** and **2**. Complete two-dimensional structures of dendrimers **1** and **2** are given in Fig. S1†.

2. Materials and methods

2.1 General procedures

All reactions were carried out in the absence of air using standard Schlenk techniques and vacuum-line manipulations when carried out in organic solvents. Commercial samples were used as received. All solvents were dried and distilled according to routine procedure before use. Thin layer chromatography was carried out on Merck Kieselgel 60F254 precoated silicagel plates. Preparative chromatography was performed on Merck Kieselgel. ^{1}H, ^{13}C, ^{31}P NMR, HMQC and HMBC measurements were performed on Bruker ARX 250, DPX 300, AV 400 and AV 500. Coupling constants are reported in Hz and chemical shifts in ppm/TMS for ^{1}H and ^{13}C. Chemical shifts for ^{31}P spectra are calibrated with phosphoric acid as an external reference. The first-order peak patterns are indicated as s (singulet), d (doublet), t (triplet), q (quadruplet). Complex non-first-order signals are indicated as m (multiplet). ^{13}C NMR signals were assigned using HMQC and HMBC sequences when required. The numbering used for NMR assignment is depicted on

Scheme 1. The following compounds have been prepared according to published procedures: julolidine-cored dendrimer **3**,[15] dendrimer **1**, dendrimer **2**,[14] dendrimer **6**.[15] The preparation of the terbutoxy-protected aminobiscarboxylate phenol derived from tyramine was adapted from described procedure.[14]

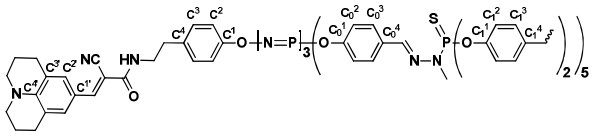

Scheme 1. Numbering scheme for NMR assignments.

Dendrimer **7**: To a solution of dendrimer **3** (200 mg, 0.104 mmol) in THF (10 mL) was added aminobis(*tert*-butyl acetate) tyramine[14] (416 mg, 1.14 mmol) and cesium carbonate (708 mg, 2.17 mmol). The solution was stirred and maintained at room temperature for 72h. The supernatant was centrifuged, filtered and evaporated to dryness under reduced pressure. The resulting crude material was diluted in THF (1 mL) and precipitated with a large amount of pentane (150 mL). The suspension was stirred for 1h at RT then the supernatant was removed by filtration. This step was repeated 5 times to afford dendrimer **7** as a yellow powder (420 mg, 65%).

^{31}P-{^{1}H} NMR ($CDCl_3$, 202.5 MHz): δ = 8.38 (s, N_3P_3); 63.11 (s, P=S); 63.22 (s, P=S).

^{1}H NMR ($CDCl_3$, 500.3 MHz): δ = 1.45 (s, 180H, O-CH_3); 1.95 (m, 4H CH_2-$\underline{CH_2}$-CH_2-N); 2.75 (m, 24H, Ph-$\underline{CH_2}$-CH_2-N and $\underline{CH_2}$-CH_2-CH_2-N); 2.92 (m, 22H, Ph-CH_2-$\underline{CH_2}$-N and $\underline{CH_2}$-CH_2-NH); 3.29 (s, 19H, N-CH_3 and CH_2-CH_2-$\underline{CH_2}$-N); 3.45 (s, 42H, N-CH_2-CO and CH_2-$\underline{CH_2}$-NH); 6.94-7.12 (m, 54H, C^2-H, $C_0{}^2$-H, C^3-H, $C_1{}^2$-H, $C_1{}^3$-H); 7.41 (s, 2H, $C^{2'}$-H); 7.61-7.66 (m, 15H, CH=N and $C_0{}^3$-H); 7.95 (s, 1H, HC=C-CN).

$^{13}C\{^1H\}$ ($CDCl_3$, 125.8 MHz): δ = 21.2 (s, CH_2-$\underline{C}H_2$-CH_2-N); 27.6 (s, $\underline{C}H_2$-CH_2-CH_2-N); 28.2 (s, O-$\underline{C}H_3$); 33.0 (s, N-$\underline{C}H_3$); 34.2 (s, Ph-$\underline{C}H_2$-CH_2-N and $\underline{C}H_2$-CH_2-NH); 41.5 (s, CH_2-$\underline{C}H_2$-NH); 50.1 (s, CH_2-CH_2-$\underline{C}H_2$-N); 56.0 (s, N-CH_2-CO, and Ph-CH_2-$\underline{C}H_2$-N); 77.0 (t, O-$\underline{C}H_3$); 80.9 (s, $\underline{C}(CH_3)_3$); C≡N signal could not be observed; 120.7 (s, C_0^2 and $C^{3'}$); 121.3 (m, C_1^2-H and C^2); 128.2 (s, C_0^3-H); 129.8 (s, C_1^3-H); 131.0 (s, C^3); 132.1 (s, C_0^4, $C^{1'}$ and $C^{2'}$); 135.7 (s, C^4); 137.1 (s, C_1^4-H); 138.7 (broad s, CH=N); 147 (s, $C^{4'}$); 148.9 (d, C_1^1); 151.2 (broad s, C_0^1 and C^1); 152.2 (s, H$\underline{C}$=C-CN); 170.6 (s, CO_2) ppm.

Dendrimer **8**: dendrimer **7** (300 mg, 0.058 mmol) was solubilized in a solution of TFA (20% in dichloromethane, 16.5 mL). The reaction mixture was stirred at room temperature for 1h and evaporated to dryness. Then ethyl acetate (15 mL) was added, stirred for 10 min at RT and evaporated to dryness. This step was repeated 8 times. The resulting powder was suspended in AcOEt (15 mL) and treated with 1 M HCl/Et_2O (1 mL) for 30 min at RT. The mixture was triturated with Et_2O (100 mL) for 15 minutes to afford a yellowish precipitate. The supernatant was removed by filtration. The resulting crude material was triturated in AcOEt (15 mL) for 30 min at RT and evaporated to dryness. This step was repeated 3 times until complete removal of TFA (^{19}F NMR) to afford dendrimer **8** (220 mg, 93%) as a yellow powder.

$^{31}P\text{-}\{^1H\}$ NMR (DMSO, 202.5 MHz): δ = 8.47 (s, N_3P_3); 62.98 (s, P=S); 63.28 (s, P=S).

^1H NMR (DMSO, 500.3 MHz): δ = 1.82 (s, 4H, CH_2-$\underline{CH_2}$-CH_2-N); 2.61 (s, 4H, $\underline{CH_2}$-CH_2-CH_2-N); 2.71 (s, 2H, $\underline{CH_2}$-CH_2-NH); 2.89 (m, 20H, Ph-$\underline{CH_2}$-CH_2-N); 3.25-3.36 (m, 37H, Ph-CH_2-$\underline{CH_2}$-N, N-CH3 and CH_2-$\underline{CH_2}$-NH); 3.86 (s, 4H, CH_2-CH_2-$\underline{CH_2}$-N); 4.03 (s, 42H, N-CH_2-CO); 6.80 (d, 2H, $C^{3'}$-H); 6.94 (d, 4H, C^2-H); 7.07 (s, 30H, C_0^2-H, C_1^2-H); 7.22 (s, 22H, and C_1^3-H and C^3-H); 7.33 (s, 2H, $C^{2'}$-H); 7.66 (m, 10H, C_0^3-H); 7.92 (d, 5H, CH=N); 8.14 (s, 1H, HC=C-CN).

$^{13}C\{^1H\}$ (DMSO, 125.8 MHz): δ = 21.1 (s, CH_2-$\underline{C}H_2$-CH_2-N); 27.5 (s, $\underline{C}H_2$-CH_2-CH_2-N); 28.2 (s, O-$\underline{C}H_3$); 30.3 (s, Ph-$\underline{C}H_2$-CH_2-N); 33.5 (d, N-$\underline{C}H_3$); 34.7 (s, $\underline{C}H_2$-CH_2-NH); 40.1 (s, CH_2-$\underline{C}H_2$-NH); 49.8 (s, CH_2-CH_2-$\underline{C}H_2$-N); 54.8 (s, N-CH_2-CO); 56.8 (s, Ph-CH_2-$\underline{C}H_2$-N); 118.1 (s, CN); 120.8 (s, C^2 and $C^{3'}$); 121.5 (s, C_0^2 and C_1^2); 128.7 (s, C_0^3); 130.6 (s, C_1^3 and C^3); 132.6 (broad, C_0^4, $C^{2'}$ and $C^{1'}$); 135.2 (s, C_1^4 and C^4); 140.8 (broad s, CH=N); 148.4 (s, $C^{4'}$); 149.2 (m, C_1^1); 151.0 (broad, C_0^1, C^1, H$\underline{C}$=C-CN); 169.2 (s, CO_2) ppm.

<u>Dendrimer **9**</u>: dendrimer **8** (220 mg, 0.054 mmol) was suspended in water (10 mL). Then a solution of sodium hydroxide (0.2 mol.L^{-1}, 5.4 mL) was added dropwise at 0°C. The resulting solution was filtered (20 µm) and freeze-dried to obtain dendrimer **9** as a yellow powder (220 mg, 90%).

$^{31}P\text{-}\{^1H\}$ NMR (D_2O/CD_3CN, 4:1, 202.5 MHz): δ = 9.51 (d, N_3P_3); 63.16 (s, P=S); 63.47 (s, P=S).

^1H NMR (D_2O/CD_3CN, 4:1, 500.3 MHz): δ = 1.69 (broad, 4H, CH_2-$\underline{CH_2}$-CH_2-N); 2.41 (s, 4H, $\underline{C}H_2$-CH_2-CH_2-N); 2.78 (s, 2H, $\underline{CH_2}$-CH_2-NH); 3.03 (m, 22H, Ph-$\underline{CH_2}$-CH_2-N, CH_2-$C\underline{H_2}$-NH); 3.30-3.53 (m, 39H, Ph-CH_2-$\underline{CH_2}$-N, N-CH_3 and $\underline{CH_2}$-CH_2-CH_2-N); 3.83 (s, 40H, N-CH_2-CO); 6.74-6.88 (m, 16H, $C^{3'}$-H, C^2-H, C_0^2-H and $C^{2'}$-H); 7.10 (s, 20H, C_1^2-H); 7.23 (s, 20H, C_1^3-H); 7.38 (d, 2H, C^3-H); 7.59 (s, 10H, C_0^3-H); 7.87 (m, 5H, CH=N).

$^{13}C\{^1H\}$ (D_2O/CD_3CN, 4:1, 125.8 MHz): δ = 29.1 (s, $\underline{C}H_2$-CH_2-CH_2-N, CH_2-$\underline{C}H_2$-CH_2-N, $\underline{C}H_2$-CH_2-NH, CH_2-$\underline{C}H_2$-NH); 32.8 (s, N-CH_3); 56.5 (s, CH_2-CH_2-$\underline{C}H_2$-N); 57.4 (s, N-CH_2-C); C≡N signal could not be observed; 121.5 (s, C_0^2, C_1^2, C^2, $C^{3'}$); 128.5 (m, C_0^2, C_0^3); 130.5 (s, C_1^3-H, C^3); 133.9 (s, $C^{1'}$, $C^{2'}$, C_0^4, C^4, C_1^4); CH=N signal could not be observed; 149.4 (m, C_0^1, C_1 and C_1^1); 150.7 (s, H$\underline{C}$=C-CN); 169.7 (s, CO_2, CO) ppm.

2.2 Computational methods

The entire simulation work was carried out using the AMBER 12 simulation package.[16] The molecular models for dendrimers **1** and **2** were created as already described.[4] Their interaction with the biomolecular target was parametrized according to a validated strategy.[17–19]

We built and simulated a molecular model of POPC lipid bilayer membrane according to a validated procedure.[20] The membrane model was constructed as composed of 144 POPC lipids with the CHARMM-GUI membrane builder[21,22] and solvated with TIP3P explicit water molecules. A suitable number of Na^+ and Cl^- ions were added into the system to reproduce the experimental ionic strength of 150 mM NaCl. The POPC lipid molecules were parametrized according to the Lipid11 force field.[20] The parameters used in the simulations are consistent with what reported previously in the literature for similar systems.[20] After initial minimization, the POPC lipid bilayer model was initially heated to 310 K (37°C) during 100 ps of MD simulation in NVT (constant number of N: atoms, V: volume, and T: temperature in the system) periodic boundary conditions. During this phase the solute was maintained as fixed. All restraints were then removed and the membrane model was equilibrated for 300 ns of MD in NPT periodic boundary conditions at the experimental temperature of 37 °C and 1 atm of pressure using semi-isotropic pressure scaling. A constant surface tension of γ=17 dyne.cm^{-1} with interfaces in the *xy* plane was applied during the MD run. During the MD simulation, the POPC bilayer reached the equilibrium showing good consistency with the experiments (area per-lipid of ≈64-67 Å^2/lipid).[20,23]

As a next step, the pre-equilibrated dendrimers **1** and **2** were put in proximity of the pre-equilibrated POPC membrane, and the obtained complex systems were again solvated in explicit water and counter ions from 150 mM NaCl. After initial minimization and heating (as described

previously), the complex systems underwent 500 ns of MD simulation in NPT periodic boundary conditions at 37 °C of temperature and 1 atm of pressure (under the conditions described above). All MD runs used a time step of 2 femtoseconds, the Langevin thermostat and an 8 Å cutoff. The long-range electrostatic effects were treated according to the particle mesh Ewald (PME) approach.[24] The SHAKE algorithm was used to treat all bonds involving Hydrogen atoms.[25] During the MD runs, the dendrimers interacted with the POPC bilayer. The time evolution of the interaction between the dendrimers and the membrane model was monitored with the *ptraj* module of AMBER 12. In particular, the number of contacts between dendrimers **1** and **2** with the POPC bilayer, and the distance between the atoms of the dendrimers (surface and core) from the lipid bilayer center were used to study the interactions and their equilibration. After ≈350 ns of simulation both systems reached the equilibrium. Additionally, the radial distribution functions – *g(r)* – of the dendrimers center of mass calculated respect to the lipid bilayer center was also obtained with the *ptraj* module of AMBER 12.

2.3 Multi-Lamellar Vesicles

MLV were prepared according to a procedure described in the literature.[26] In a round bottom flask the DPPC or DPPC/POPC:75/25 powder was dissolved in pure chloroform. The solvent was evaporated to dryness under reduced pressure at room temperature. The resulting dried film of phospholipids was rehydrated with an appropriate amount of PBS solution and was cooled in liquid nitrogen until frozen then heated at a temperature of 52°C (above the main transition temperature) for 30 minutes. This protocol was performed five times in a raw; the resulting suspension was then stored at 4°C. In normal physiological conditions, monocytes present an average diameter superior to 15 μm^2 whereas generation 1 PPH dendrimers have a mean diameter around 2 to 3 nm in aqueous solutions. The order of magnitude of the average size and

the concentrations of MLV in the buffer medium were then determined so as to be as relevant as possible, taking into account the size of monocytes and the dendrimer concentration used in a typical monocyte activation experiment, *i.e.*, 20 µM *ex vivo*. Dynamic Light Scattering (DLS) technique was employed to measure the hydrodynamic radius of the MLV in 10-fold, 15-fold and 20-fold diluted samples of DPPC and DPPC/POPC:75/25 suspensions. The systems were found to be very heterogeneous, showing the presence of a population with an average size between 3.5 and 4.5 µm, and the presence of populations with sizes superior to 10 µm, which is the instrumental limit of detection. Despite this heterogeneity, the difference was considered as acceptable for this model system. In a 30 mM suspension, the concentration of vesicles measured with a hemocytometer by optical microscopy was found to be in the order of 10^8 vesicles.mL^{-1}. Assuming a monocyte concentration of 1.5 million cells.mL^{-1} in monocyte activation experiments typically run at a 20 µM dendrimer concentration,[5] the final dendrimer/monocyte ratio in *ex vivo* cultures was supposed to be about 10^{-14} mol.cell^{-1}. A suitable dendrimer/MLV ratio of 3.10^{-14} mol.vesicle^{-1} was obtained with 30 mM suspensions of phospholipids containing 10% molar ratio (3.10^{-6} mol.mL^{-1}) of dendrimer.

2.4 Differential Scanning Calorimetry

Prior to DSC analyses, MLV suspensions were diluted with PBS (to register thermograms of pure MLV) or with dendrimer-buffer solutions (to investigate MLV-dendrimer systems) to a DPPC or DPPC/POPC:75/25 final concentration of 30 mM. The DSC technique was first optimized on pure DPPC suspensions in order to determine the DPPC concentration at which the main transition peak is strong enough to allow retrieval of reliable calorimetric data. A 30 mM concentration of DPPC and of DPPC/POPC:75/25 in the sample was found to be optimal to study the transition signal during heating to maximal temperature at v=1°.min^{-1} (T_m).

Extrapolated maximal temperature at $v=0°.min^{-1}$ (T_m, v=0) and endothermic ΔH were measured as the area under the curve for each heating cycle and normalized per mole of phospholipid. Main DSC experiments were run on 30 μL of phospholipid suspensions and dendrimer-phospholipid mixtures at 10% molar ratio; samples were put in aluminum crucibles, sealed with lid; an empty crucible was used as reference. All analyses were performed with a Perkin-Elmer Differential Scanning Calorimeter, in a temperature range between 10°C and 60°C; six heating/cooling cycles were programmed, the first two at a scanning rate of 20°/min and 10°/min (for sample equilibration and exemption of thermal history) and the subsequent four at a rate of 1°/min; isothermic steps of 10 min at 10°C were also programmed between heating/cooling cycles. Thermograms and calorimetric data were elaborated and calculated by the Perkin Elmer "Pyris Series" software.

2.5 PBMC purification

Fresh blood samples were collected by the "Etablissement Français du Sang", the only institution accredited for blood sampling in France. Scientific experimentation with human material were conducted according to EU treaties ETS N. 164 of 04/04/1997 and ETS N. 168 of 12/01/1998 (additional protocol), regulating the protection of human rights and dignity of the human being in Biology and Medicine. Accordingly, informed consent of healthy donors for research purpose was obtained, and the identity as well as any other type of information regarding blood donors have been treated as strictly confidential. Procedures to ensure protection and confidentiality of data were based on anonymity of samples.

PBMC were prepared on a Ficoll-Paque density gradient (Amersham Biosciences AB, Upsalla, Sweden) by centrifugation (800 g, 30 min at room temperature). Collected PBMC were washed twice and finally diluted at 1.5 million cells per mL in complete RPMI 1640 medium,

i.e., supplemented with penicillin and streptomycin, both at 100 U per mL (Cambrex Bio Science, Verviers, Belgium), 1 mM sodium pyruvate and 10% heat-inactivated fetal calf serum (both from Invitrogen Corporation, Paisley, UK).

2.6 Monocyte purification and culture

Highly pure $CD14^+$ monocytes (over 95%, as checked by flow cytometry) were negatively selected from PBMC by magnetic cell sorting (Dynabeads Untouched Human Monocytes, Invitrogen Dynal AS, Oslo, Norway) according to the manufacturer's instruction manual. Purified monocytes were diluted at 1.5 million cells per mL in complete RPMI 1640 medium.

2.7 Bioactivity of dendrimers

2.10^5 monocytes were cultured in 200 µL of complete RPMI 1640 medium in a 96-well plate for 72 to 96 hr. Dendrimers **1** (positive control), **2**, **6** or **9** were added at the beginning of the cultures at the specified concentration, between 1 and 50 µM. Morphological changes, and thus activation of monocytes, were analyzed by flow cytometry using a FACS-Scan cytometer (BD Biosciences, San Jose, CA, USA).

2.8 Quantification of the binding of dendrimers on monocyte cell surface

To assess the total binding of dendrimers, purified monocytes were incubated for 30 min at 4°C with fluorescent dendrimers **6** or **9** at the specified concentrations. The binding was quantified by flow cytometry as the mean fluorescence intensity (mfi) of the monocytes (FACS-Scan cytometer). The mfi base line was quantified with purified monocytes incubated with dendrimers **1** or **2** in the same conditions. This mfi value was subtracted from the mfi measured on monocytes incubated with fluorescent dendrimers.

The non-specific binding was quantified as follows: in a first step, purified monocytes were incubated for 15 min at 4°C with 200 µM of dendrimers **1** or **2**, then the specified concentrations of dendrimers **6** and **9** were added for 15 min at 4°C. Cells were extensively washed before flow cytometry analysis which was used for quantification of mfi.

The specific binding was calculated by subtracting the non-specific binding from the total binding.

For the competition binding: in a first step, purified monocytes were incubated for 15 min at 4°C with 50 µM of dendrimer **6**, then the specified concentrations (between 10 nM and 1 mM) of dendrimer **1** were added for 15 min at 4°C. Cells were extensively washed before flow cytometry analysis which was used for quantification of mfi.

2.9 Internalization of dendrimers by monocytes

Purified monocytes were incubated for 30 min at 37°C with fluorescent dendrimers **6** or **9** at 20 µM. Internalization was assessed using a LSM 510 confocal microscope (Carl Zeiss, Iena, Germany) equipped with the 63X lense (ON 1.4 Plan-Apo) with a (x2) numeric zoom. Images were implemented with the LSM Image Browser software.

3. Results and discussion

3.1 Chemical syntheses of relevant fluorescent nanomolecular tools

Fluorescently labelled dendrimers **6** and **9**, analogues of dendrimers **1** and **2** respectively, have been designed to visualize the interactions of PPH dendrimers with the cell membrane of monocytes. For this purpose, a common strategy consists in grafting stochastically a fluorescent

probe onto the surface of the dendrimer target, resulting in the production of a population of dendrimers.[27] This stochastic approach, albeit time-saving, suffers from two major drawbacks which are i) the obtaining of stochastic objects which are not easily characterized, ii) the presence of the fluorescent probe on the biologically interacting surface of the dendrimer which might alter the biological response. Oppositely, the core labelling strategy that has been developed in previous synthetic approaches might appear much more tedious to achieve,[28] but this option results in perfectly defined dendrimeric molecules. Consequently, we have designed dendrimer **9**, the fluorescent analogue of dendrimer **2**, using the strategy which has been used to design dendrimer **6**, the fluorescent analogue of dendrimer **1** (Scheme 2).[15] The synthetic approach relies on a fluorescent dendrimeric synthon **3** having a julolidine derivative at the core and $PSCl_2$ surface functions. Dendrimer **3** is obtained from hexachlorocyclotriphosphazene by controlling the number of nucleophilic substitution of the chlorine atoms with a phenol bearing a julolidine-derived tag.[15] Its surface is modified by nucleophilic substitution of the chlorine atoms by a *tert*-butoxy-protected carboxylic acid-based phenol derived from tyramine in the presence of cesium carbonate in THF. The reaction is easily monitored by ^{31}P NMR, as for other PPH dendrimers.[29] The dissymmetry of the dendrimer **7** is evidenced on the ^{31}P NMR spectrum by the presence of two singlets at 63.1 (major) and 63.2 (minor) ppm in almost a 3 to 2 ratio, corresponding to the phosphorous atoms located at the divergent point and occupying the half spaces separated by the cyclotriphosphazene. A significant broadening of typical signals of the thiophosphorhydrazone branches is also observed on the ^{1}H and ^{13}C-$\{^{1}H\}$ NMR spectra. Following *tert*-butoxy deprotection, the dissymmetry is also traduced on the ^{31}P NMR spectrum of the resulting polycarboxylic acid dendrimer **8,** and its sodium salt **9,** by a set of two singlets at 62.98 and 63.28 ppm, and 63.16 and 63.47 ppm, respectively. As previously described in a

previous study,[14] the PPH scaffold is not affected by the *tert*-butoxy removal procedure. Contrarily, the julolidine moiety was found to be rather sensitive to the conditions of reaction. As a consequence, we were unable to completely remove the *tert*-butoxy groups. Approximately 3% of *tert*-butoxy groups were found to be uncleaved following the optimized procedure of deprotection, as traduced by the presence of a typical signal at 1.39 ppm on the ^{1}H NMR spectrum of **8**.

Scheme 2. Synthesis of fluorescent analogs of dendrimers **1** (dendrimer **6**) and **2** (dendrimer **9**).

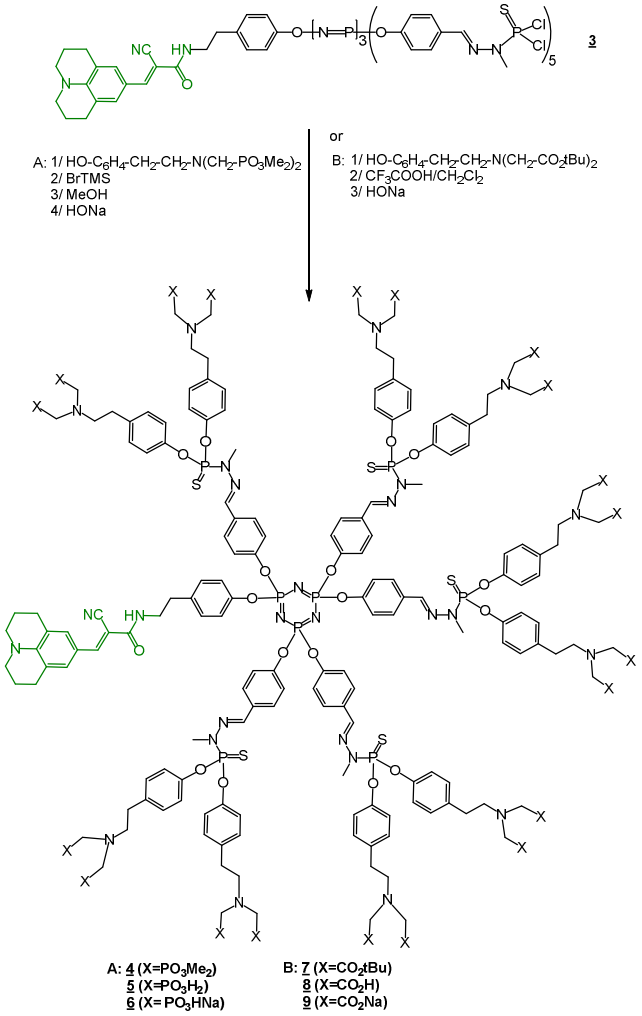

3.2 All-atom MD simulations show superficial adsorption of the PPH dendrimers with a lipid bilayer

To obtain a predictive description of the interaction between the dendrimers and a lipid bilayer at a detailed molecular level, we have employed all-atom Molecular Dynamics (MD) simulations of dendrimers **1** and **2** in the presence of a POPC membrane model. We have recently reported all-atom MD simulations of dendrimer **1** in solution at 37°C in presence of explicit water molecules and NaCl (150 mM).[4] A similar molecular model of dendrimer **2** was created for the study (Fig. 2). A molecular model of a portion of membrane composed of 144 POPC lipids was initially equilibrated for 300 ns of MD simulation in NPT (constant number of N: atoms, P: pressure, and T: temperature in the system) periodic boundary conditions in a solution containing explicit water molecules and the suitable number of Na^+ and Cl^- ions to reproduce the physiological and experimental NaCl concentration of 150 mM. During this time, the POPC membrane reached the equilibrium with good stability, and converged to an area per-lipid of ≈64–67 $Å^2$/lipid (Fig. S3†), in optimal consistency with the experimental values.[20,23] Dendrimers **1** and **2**, pre-equilibrated in solution, were put in proximity of the pre-equilibrated POPC bilayer as shown in Figure 2a, and the obtained complex systems were again solvated with explicit water molecules and Na^+ Cl^- ions. Both systems underwent 500 ns of unbiased all-atom MD simulation in NPT conditions. All systems reached the equilibrium in the MD regime after ≈350 ns of simulation. During the MD runs, dendrimers **1** and **2** interact with the lipid bilayer (Fig. 2b): first intermittently, during the first ≈150 ns, and then more stably, as it is demonstrated in Figure 2c by the number of intermolecular POPC-dendrimer contacts as a function of simulation time. In fact, after ≈150 ns both dendrimers undergo structural rearrangement attempting to fit their hydrophobic core in the interior of the lipid bilayer, and leaving the hydrophilic and negatively

charged surface groups exposed to the external solution. Since this behavior is revealed during unbiased MD simulations, this is representative of the spontaneous interaction of the dendrimers with the POPC membrane.

Figures 2b and d show similar mechanisms of penetration for both dendrimers based on local adsorption of the hydrophobic core into the bilayer. This effect was quantified by extracting

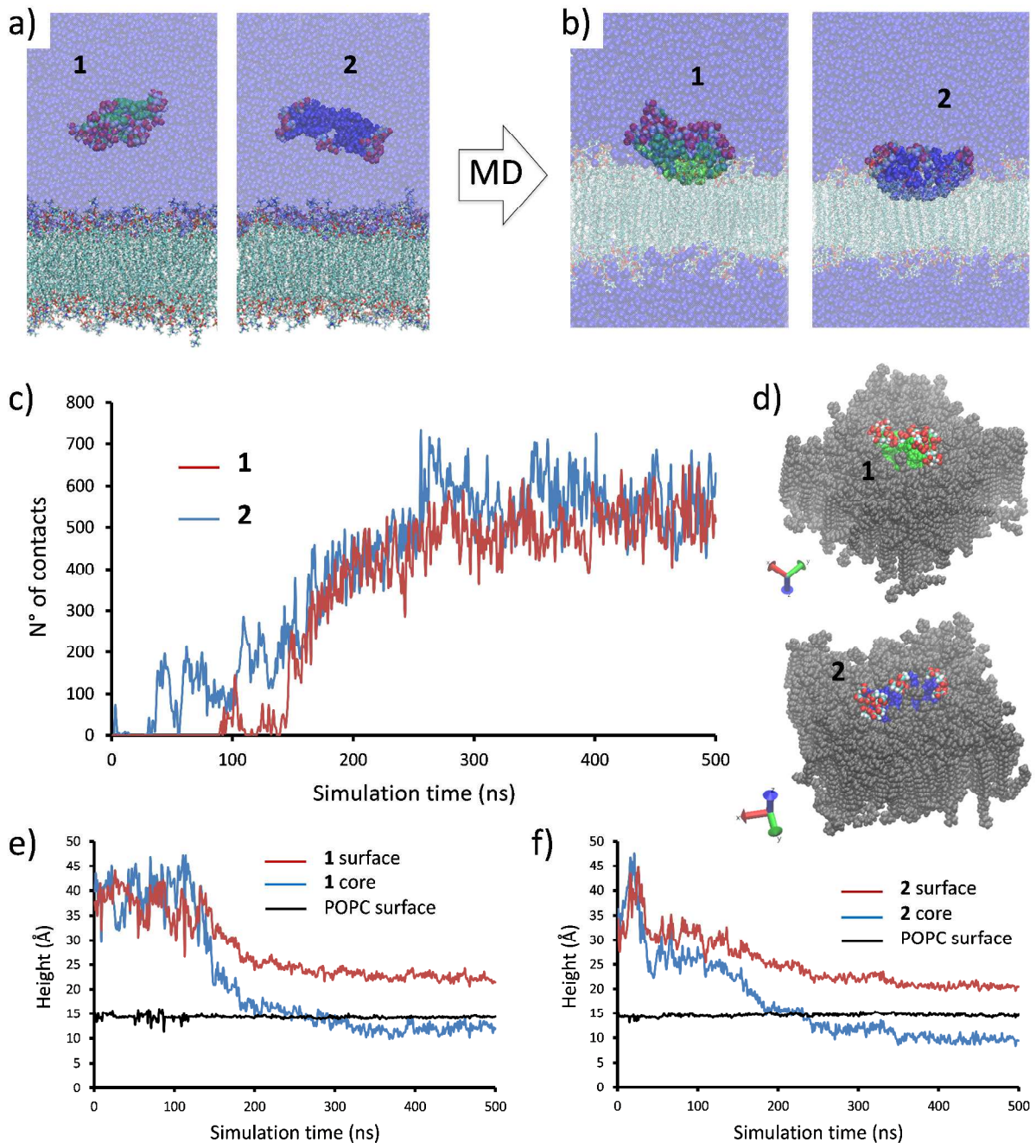

Fig. 2 Modeling the non-specific interaction between dendrimers and lipid bilayer in solution. (a) Initial configurations of the complex simulated systems containing dendrimers **1** and **2** in the presence of a portion of POPC membrane (transparent blue). (b) Equilibrated (final) configurations of the simulated systems. (c) Number of contacts between the dendrimers and the POPC membrane model at variance of the simulation time. (d) Top view of the interaction site (dendrimer **1** in green, dendrimer **2** in blue). (e,f) Assessing the mechanisms of interaction: after initial intermittent interaction, the two dendrimers are adsorbed on the POPC bilayer surface. In black: average height of the lipid heads (center of mass). In particular, the hydrophilic surface groups stay exposed to the solvent, while the hydrophobic core is locally adsorbed inside the lipid bilayer.

from the MD trajectories the average distances between the dendrimers surface (red) and core (blue) atoms from the center of the lipid bilayer (height equal to 0 in Fig. 2e and f). It is interesting to compare the surface and core atoms displacement with the position of the lipid phosphorylated head groups (Fig. 2e and f: black). The data provide a picture of the structural reorganization occurring after ≈150-200 ns of MD simulation, where the hydrophobic core is locally absorbed in the POPC membrane. The negatively charged surface groups of the dendrimers (Fig. 2b and d: red) act as "umbrellas", limiting dendrimers penetration into the membrane. Since the surface groups of dendrimer **2** are smaller than those of dendrimer **1**, this produces a slightly deeper penetration of dendrimer **2** in the bilayer, albeit this difference is very subtle.

The radial distribution functions *g(r)* of the dendrimers center of mass respect to the bilayer surface (phosphorylated head groups) were also calculated from the MD trajectories (Fig. S4†). The *g(r)* of dendrimers **1** and **2** respect to the lipid bilayer center is found to be very similar, suggesting that the non-specific interactions of the two dendrimers with the POPC membrane are nearly the same, and that these are, in general, very weak.[17,18,30] Thus, the MD simulations depict the non-specific interaction between the dendrimers and the lipid bilayer as local and superficial.

3.3 DSC experiments confirm only weak non-specific interaction of the PPH dendrimers with lipid bilayers

The different surface functions generated on the four dendrimers could evidently affect the physicochemical behavior thereof as well as the cell/dendrimer interaction phenomenon. Therefore, we have undertaken a physicochemical characterization of the four dendrimers involved in this study. The zeta potential of the dendrimer is considered to be essential to the

adsorption on the negative cell membrane.[31] We have determined that all dendrimers have strongly negative zeta potential of -55 mV for dendrimers **1** and **6** and -35 mV for dendrimers **2** and **9**. Since most biological cells have negative zeta potentials, it is likely that the four dendrimers with also significantly negative zeta potentials are not able to stick non-specifically to cells but can most probably interact through a receptor-mediated interaction that allows their binding only when the receptor-ligand interaction is strong enough to overcome electrostatic repulsions. Moreover, these values combined with the measurement of the mean hydrodynamic diameters, at around 4 and 6 nm in solution for all dendrimers, show that they all have a good stability in solution and do not aggregate at the concentrations used for biological experiments. Then, information regarding the interactions of dendrimers **1** and **2** with phospholipid bilayers were evaluated from the modifications in the thermotropic behavior of pure DiPalmitoyl PhosphatidylCholine (DPPC) and mixed DPPC/POPC:75/25 (POPC: 1-Palmitoyl, 2-Oleyl PhosphatidylCholine) multi-lamellar vesicles (MLV) measured by Differential Scanning Calorimetry (DSC, Table 1).

Table 1 Main transition calorimetric data[a] for MLV suspensions of DPPC/POPC:75/25 (30 mM) alone, and with dendrimers **1**, **2**, **6** or **9** (3 mM).

	Scan number	T_m (°C)	ΔH[b]
MLV alone	1st	37.93	-4.37
	4th	37.96	-4.30
MLV + **1**	1st	37.99	-3.72
	4th	38.04	-3.65
MLV + **6**	1st	37.33	-3.66
	4th	37.54	-3.72
MLV + **2**	1st	38.07	-3.57
	4th	38.15	-3.63
MLV + **9**	1st	38.50	-3.75
	4th	38.65	-3.75

[a] Values are given for heating cycles. Cooling cycles gave comparable absolute values. [b] ΔH: transition enthalpy normalized per mole of phospholipid. Unit is $kcal.mol^{-1}$.

DSC is a technique used to probe alterations of the bilayer structure induced by external substances, such as possible dendrimer incorporation. These alterations include variations in the spacing among polar head groups and penetration into the lipophilic environment composed by alkyl chains.[32] They result in the modification of the calorimetric values such as the maximal temperature (T_m) and the endothermic variation of the enthalpy of transition (ΔH) accompanying the transition from the gel phase to the liquid crystal phase. The optimal concentration of phospholipids used to prepare MLV was determined at 30 mM, and the ratio between phospholipids and dendrimers at 10 to 1 (see experimental details). Whatever the dendrimer added to MLV, the main transition peak is weakly affected (Fig. S2†), as shown by very low thermotropic changes in T_m and small enthalpy changes of the gel to liquid-cristalline phase transition of the bilayers. No variation of the thermodynamic values is observed between the 1st and the 4th scan, both in pure DPPC (Table S1†) and DPPC/POPC:75/25 MLV (Table 1). Moreover, the reduction of ΔH from 4.30 kcal.mol^{-1} for DPPC/POPC:75/25 MLV alone to about similar values of 3.70 ± 0.05 kcal.mol^{-1} for all the MLV/dendrimer mixtures is very low compared to previous work with PAMAM dendrimers incorporation in DPPC lipid bilayers.[32] These results tend to demonstrate that the non-specific interactions between the four dendrimers and a simplified model of the cell membrane are very weak or that the dendrimers do not deeply penetrate in the phospholipidic bilayer. Hence, these experimental data are consistent with the predictive all-atom MD simulations performed with dendrimers **1** and **2**.

3.4 Biological binding studies demonstrate specific interaction of the ABP-capped PPH dendrimer with monocytes

In order to screen the biological properties of these dendrimers, a biological test for monitoring the activation of human monocytes *in vitro* has been developed. Monocytes are white blood cells playing multiple roles in the immune system, in particular in response to anti-inflammatory signals.[33] One of the first morphological features indicating the activation of monocytes is an increase of their size and granularity.[34] These changes appear within a few days in *in vitro* cultures of monocytes, and can be visualized by flow cytometry. We have conducted this test with the four dendrimers at concentrations between 1 and 50 μM (Fig. 3). Dendrimers **1** and **6** activate human monocytes at the concentration of 5 μM and above, a slight shift toward the higher concentration may be noticed with dendrimer **6**. Conversely, dendrimers **2** and **9** do not activate these cells as no morphological change is induced, even though activated monocytes can be observed occasionally, depending on the donor. Regarding the stimulus they sense, monocytes commit to either an inflammatory or an anti-inflammatory activation. These are characterized by specific changes at the transcriptional,[35] phenotypical,[5] and functional levels.[36]

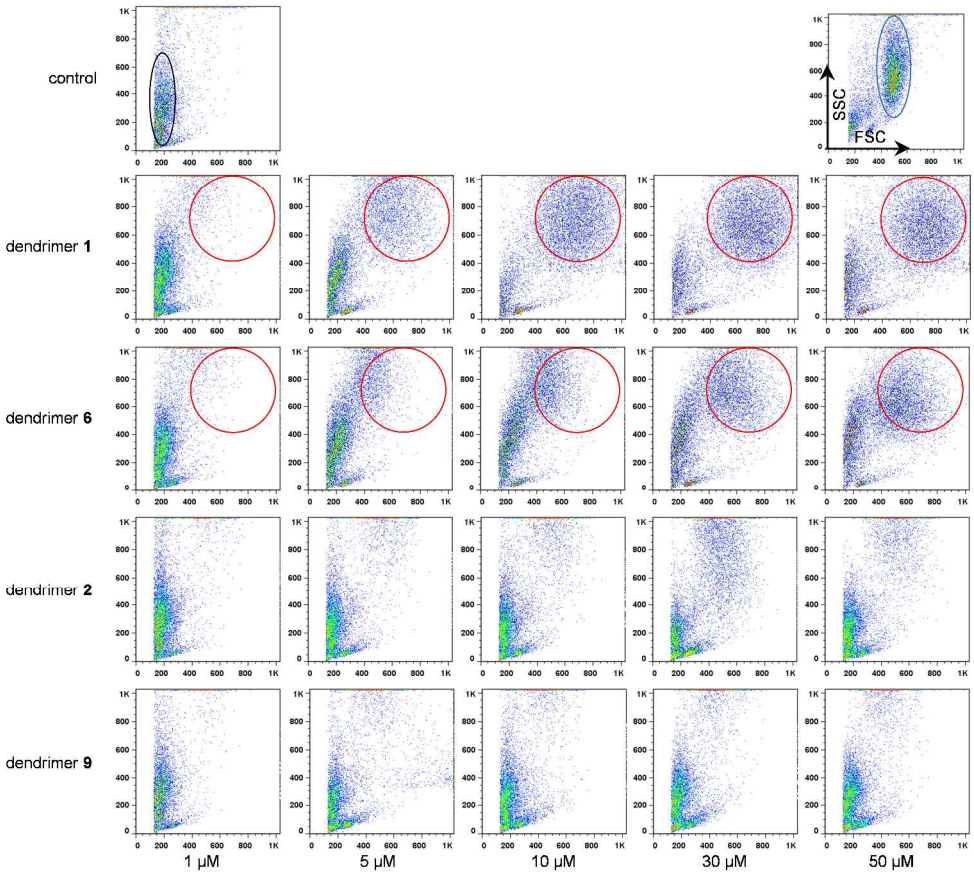

Fig. 3 Flow cytometry analyses of morphological changes (size – the Forward Scatter (FSC) parameter on the *x*-axis – and granularity – the Side Scatter (SSC) parameter on the *y*-axis – criteria) undergone by purified human monocytes in the presence of the different dendrimers at the indicated concentration. The monocytes purified at day 0 are shown in the upper right dot plot (surrounded in the blue ellipse). At day 6, the black ellipse in the upper left dot plot identifies died or dying monocytes, while the activated monocytes are circled in red. Data are from one representative experiment out of three.

When monocytes are triggered by dendrimers **1** and **6**, we show that typical markers of an anti-inflammatory activation, namely mannose receptor MRC1 and interleukin(IL)-10, are significantly up-regulated at the mRNA level, whereas IL-12 (a typical inflammatory cytokine) is not modified. On the contrary, dendrimers **2** and **9** do not modify the level of expression of these markers (Fig. 4a). The same dichotomy between dendrimers **1** and **6**, and dendrimers **2** and **9** is observed regarding the phenotype of monocytes which significantly down-regulate the

expression of proteins such as HLA-DR (MHC class II molecules) and CD14 when they are activated by azabisphosphonate dendrimers (Fig. 4b), as we have already shown.[5,15] Thus, all together, these results show that dendrimers **1** and **6** induce an anti-inflammatory activation of human monocytes *in vitro*, as expected. Oppositely, dendrimers **2** and **9** are inactive on these cells. Therefore, they constitute negative controls of the bio-active dendrimers for the binding experiments on human monocytes.

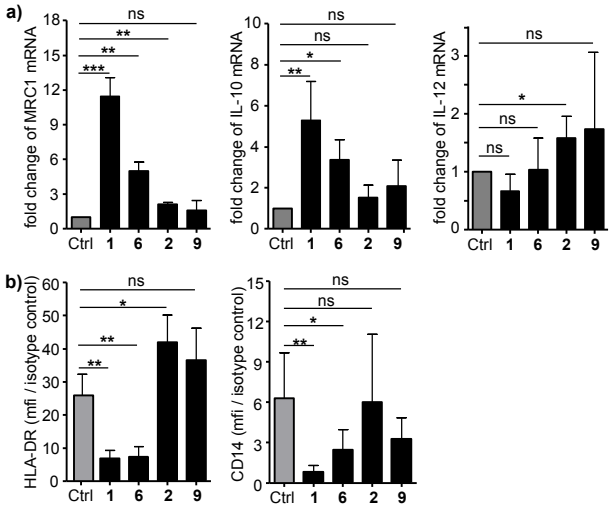

Fig. 4 (a) qRT-PCR of mRNA expression for MRC1, IL-10 and IL-12 in monocytes stimulated with dendrimers **1**, **6**, **2** and **9**. Expression levels are normalized to the GAPDH mRNA. Relative expressions are calculated using the ΔΔCt method, and results represent the n-fold regulation induced by dendrimers in comparison with non-stimulated control monocytes (n=1). Data are expressed as mean ± SD from 3 independent experiments. *, $p < 0.05$; **, $p < 0.01$; ***, $p < 0.001$, one-tail paired Student's t-test. (b) Flow cytometry analysis of the cell-surface expression of HLA-DR and CD14. Data are expressed as medians ± SD from 5 independent experiments. *$p<0.05$, **$p<0.01$ (Mann-Whitney's test).

For saturation binding assays, human monocytes have been incubated with the fluorescent dendrimers **6** and **9** in increasing concentrations, at 4°C to avoid internalization of the molecules. This has been checked by confocal microscopy (data not shown). The binding of these probes at the surface of monocytes has been quantified by flow cytometry, measuring the mean

fluorescence intensity (mfi) of the cell population. For each of the three independent donors that have been tested, dendrimer **6** and dendrimer **9** show quite different pattern of binding (Fig. 5).

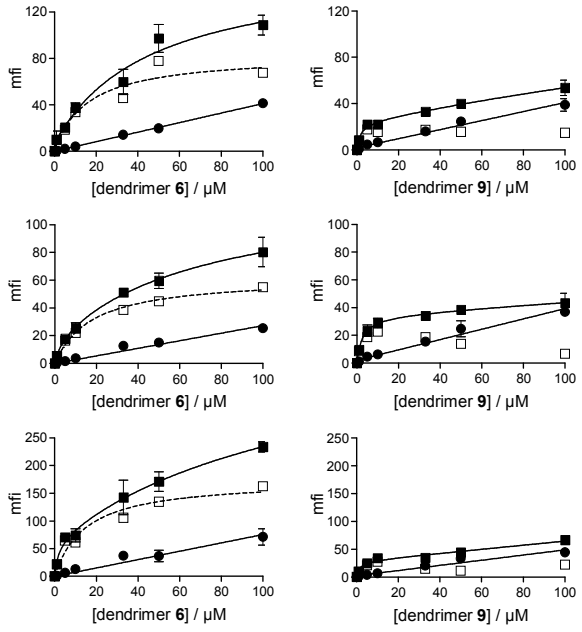

Fig. 5 Black squares show the total binding of dendrimers **6** (left graphs) and **9** (right graphs) on monocytes of three independent donors (the two graphs for one donor are on a row). Black circles show the non-specific binding, and white squares show the calculated specific binding of dendrimer **6**. For each donor and concentration, the symbols represent the mean ± SD of triplicates.

The total binding of dendrimer **6** fits a logarithmic curve, unlike that of dendrimer **9**. Nevertheless, binding of dendrimer **6** does not reach a saturation asymptote, suggesting that both specific and non-specific binding components are involved. To discriminate between both, we have performed a second binding assay in which the surface of monocytes is saturated with dendrimer **1**, then dendrimer **6** is added with increasing concentration. In this setting the non-specific binding of dendrimer **1** is displaced by dendrimer **6**, therefore it can be quantified by flow cytometry. Then, the level of the non-specific binding is subtracted from the mfi of the total binding to give the specific binding (Fig. 5). The calculated curve for dendrimer **6** fits with a

typical saturation asymptote reflecting a specific binding component, likely mediated by surface receptor(s). The K_d of dendrimer **6** is estimated thereof at 16 μM. Using the same experimental setting with dendrimers **2** and **9**, we show that the non-specific binding corresponds to the total binding for these inactive molecules (Fig. 5). Finally, a competitive binding assay between dendrimer **6**, incubated in a first step, and dendrimer **1**, added with increasing concentrations in a second step, is performed. If the concentration of dendrimer **1** is plotted as decimal logarithm, the typical sigmoid curves that are obtained (Fig. 6) enable the determination of the K_i of dendrimer **1** (K_i = 12 μM).[37] This K_i value can be considered the K_d of dendrimer **1**. On the all, dendrimers **1** and **6** have similar biological properties and comparable K_d values. These points confirm the relevance of designing an analogue of dendrimer **1** by grafting a fluorescent tag on the core of the molecule, far from the surface.

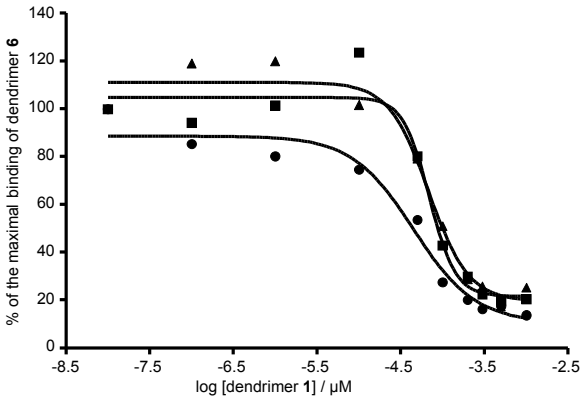

Fig. 6 Competitive binding assay between dendrimer **6** and dendrimer **1** on human monocytes. Results are expressed as means of triplicates from three independent donors.

Using confocal microscopy, we show that dendrimer **6** is internalized by human monocytes, whereas dendrimer **9** is not. The latter stays bound at the membrane (Fig. 7 and Supplementary Movies). Consequently, the specific binding followed by the internalization of dendrimers **1** and **6** by human monocytes leading to anti-inflammatory activation of cells can be

unambiguously correlated to the presence of azabisphosphonate groups at the periphery of the dendritic scaffold. On the contrary, the carboxylate terminated PPH dendrimers **2** and **9** do not specifically bind to the cell surface of monocytes, they are not internalized and do not activate monocytes.

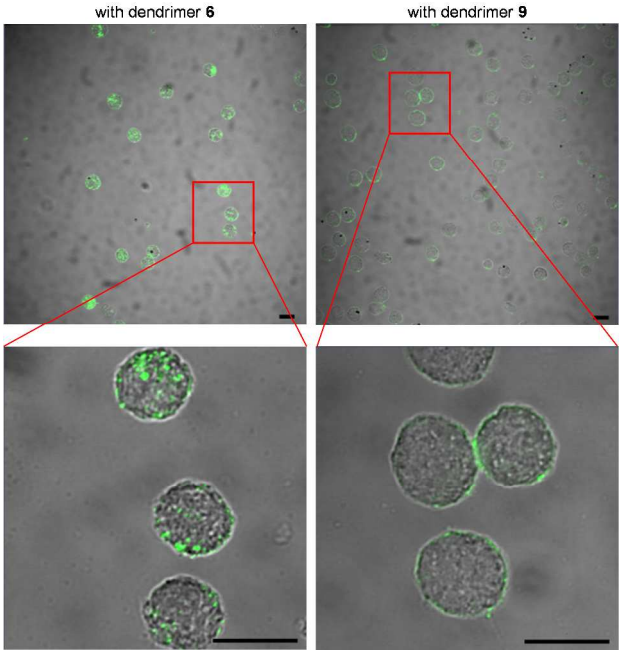

Fig. 7 Confocal microscopy shows internalization of dendrimer **6** (upper left image and zoom below) whereas dendrimer **9** binds non-specifically to monocytes and is not internalized (upper right image and zoom below). The dark bars represent 10 μm.

4. Conclusion

We have used a multidisciplinary approach to prove that an anti-inflammatory PPH dendrimer capped with azabisphosphonate end groups (dendrimer **1**) interacts both non-specifically and specifically with human monocytes. The non-specific interaction is due to a weak, local, and superficial adsorption of the molecule on the phospholipidic bilayer; it also occurs with an inactive PPH dendrimer (capped with azabiscarboxylate end groups, dendrimer

2). The specific interaction occurs with K_d value of 12 μM and leads to recognition by and activation of human monocytes. Therefore, this specific recognition involves one or several receptor(s), the identification of which is ongoing. Several types of dendrimers have shown anti-inflammatory properties *per se*.[38–43] In most cases, the receptors involved in the recognition of these nanomolecules remain unknown. This is not the case when dendrimers have been rationally designed to target and be recognized by a given receptor[40,42] or a given cluster of receptors.[39] Isolation, purification and identification of the receptor(s) involved in the recognition of azabisphosphonate-capped PPH dendrimers by human monocytes is a challenging ongoing issue.

Acknowledgments

CNRS, INSERM, university Paul Sabatier of Toulouse are acknowledged for institutional funding. We thank Sophie Allart for technical assistance at the cellular imaging facility of INSERM 1043, Toulouse. This research work was supported by the French “Fondation pour la Recherche Médicale” (FRM), 2011 call “Chemistry for Medicine” DCM20111223039.

Abbreviations

DLS, dynamic light scattering; DPPC, DiPalmitoyl PhosphatidylCholine; DSC, differential scanning calorimetry; FSC, forward scatter; IL, interleukin; MLV, multi-lamellar vesicles; MD, molecular dynamics; NPT, constant number of N: atoms, P: pressure, and T: temperature; NVT, constant number of N: atoms, V: volume, and T: temperature; POPC, 1-Palmitoyl, 2-Oleyl PhosphatidylCholine; SSC, side scatter.

References

1 V. Wagner, A. Dullaart, A. K. Bock and A. Zweck, The emerging nanomedicine landscape, *Nat. Biotechnol.*, 2006, **24**, 1211–1217.

2 M. Mammen, S. K. Choi and G. M. Whitesides, Polyvalent interactions in biological systems: implications for design and use of multivalent ligands and inhibitors, *Angew. Chem. Int. Ed.*, 1998, **37,** 2754–2794.

3 R. M. Kannan, E. Nance, S. Kannan and D. A. Tomalia, Emerging concepts in dendrimer-based nanomedicine: from design principles to clinical applications, *J. Intern. Med.*, 2014, **276**, 579-617.

4 A. M. Caminade, S. Fruchon, C. O. Turrin, M. Poupot, A. Ouali, A. Maraval, M. Garzoni, M. Maly, V. Furer, V. Kovalenko, J. P. Majoral, G. M. Pavan and R. Poupot, The key role of the scaffold on the efficiency of dendrimer nanodrugs, *Nat. Commun.*, 2015, **6**, 7722.

5 M. Poupot, L. Griffe, P. Marchand, A. Maraval, O. Rolland, L. Martinet, F. E. L'Faqihi-Olive, C. O. Turrin, A. M. Caminade, J. J. Fournié, J. P. Majoral and R. Poupot, Design of phosphorylated dendritic architectures to promote human monocyte activation, *FASEB J.*, 2006, **20**, 2339–2351.

6 S. Fruchon, M. Poupot, L. Martinet, C. O. Turrin, J. P. Majoral, J. J. Fournié, A. M. Caminade and R. Poupot, Anti-inflammatory and immunosuppressive activation of human monocytes by a bioactive dendrimer, *J. Leukoc. Biol.*, 2009, **85**, 553–562.

7 D. Portevin, M. Poupot, O. Rolland, C. O. Turrin, J. J. Fournié, J. P. Majoral, A. M. Caminade and R. Poupot, Regulatory activity of azabisphosphonate-capped dendrimers on

human CD4+ T cell proliferation enhances ex-vivo expansion of NK cells from PBMCs for immunotherapy, *J. Transl. Med.*, 2009, **7**, 82.

8 P. Marchand, L. Griffe, M. Poupot, C. O. Turrin, G. Bacquet, J. J. Fournié, J. P. Majoral, R. Poupot and A. M. Caminade, Dendrimers ended by non-symmetrical azadiphosphonate groups: synthesis and immunological properties, *Bioorg. Med. Chem. Lett.*, 2009, **19**, 3963–3966.

9 L. Griffe, M. Poupot, P. Marchand, A. Maraval, C. O. Turrin, O. Rolland, P. Métivier, G. Bacquet, J. J. Fournié, A. M. Caminade, R. Poupot and J. P. Majoral, Multiplication of human natural killer cells by nanosized phosphonate-capped dendrimers, *Angew. Chem. Int. Ed.*, 2007, **46**, 2523–2526.

10 M. Hayder, M. Poupot, M. Baron, D. Nigon, C. O. Turrin, A. M. Caminade, J. P. Majoral, R. A. Eisenberg, J. J. Fournié, A. Cantagrel, R. Poupot and J. L. Davignon, A phosphorus-based dendrimer targets inflammation and osteoclastogenesis in experimental arthritis, *Sci. Transl. Med.*, 2011, **3**, 81ra35.

11 S. Fruchon, A. M. Caminade, C. Abadie, J. L. Davignon, J. M. Combette, C. O. Turrin and R. Poupot, An azabisphosphonate-capped poly(phosphorhydrazone) dendrimer for the treatment of endotoxin-induced uveitis, *Molecules*, 2013, **18**, 9305–9316.

12 X. Bosch, Dendrimers to treat rheumatoid arthritis, *ACS Nano*, 2011, **5**, 6779–6785.

13 S. Fruchon, S. Mouriot, T. Thiollier, C. Grandin, A. M. Caminade, C. O. Turrin, H. Contamin and R. Poupot, Repeated intravenous injections in non-human primates demonstrate preclinical safety of an anti-inflammatory phosphorus-based dendrimer, *Nanotoxicology*, 2015, **9**, 433–441.

14 O. Rolland, C. O. Turrin, G. Bacquet, R. Poupot, M. Poupot, A. M. Caminade and J. P. Majoral, Efficient synthesis of phosphorus-containing dendrimers capped with isosteric functions of amino-bismethylene phosphonic acids, *Tetrahedron Lett.*, 2009, **18**, 2078–2082.

15 O. Rolland, L. Griffe, M. Poupot, A. Maraval, A. Ouali, Y. Coppel, J. J. Fournié, G. Bacquet, C. O. Turrin, A.M. Caminade, J. P. Majoral and R. Poupot, Tailored control and optimisation of the number of phosphonic acid termini on phosphorus-containing dendrimers for the ex-vivo activation of human monocytes, *Chem–Eur. J.*, 2008, **14**, 4836–4850.

16 D. A. Case, T. A. Darden, T. E. Cheatham III, C. L. Simmerling, J. Wang, R. E. Duke, R. Luo, R. C. Walker, W. Zhang, K. M. Merz, B. Roberts, S. Hayik, A. Roitberg, G. Seabra, J. Swails, A. W. Götz, I. Kolossváry, K. F. Wong, F. Paesani, J. Vanicek, R. M. Wolf, J. Liu, X. Wu, S. R. Brozell, T. Steinbrecher, H. Gohlke, Q. Cai, X. Ye, J. Wang, M. J. Hsieh, G. Cui, D. R. Roe, D. H. Mathews, M. G. Seetin, R. Salomon-Ferrer, C. Sagui, V. Babin, T. Luchko, S. Gusarov, A. Kovalenko and P. A. Kollman, AMBER 12, 2012, University of California, San Francisco.

17 D. A. Torres, M. Garzoni, A. V. Subrahmanyam, G. M. Pavan and S. Thayumanavan, Protein-triggered supramolecular disassembly: insights based on variations in ligand location in amphiphilic dendrons, *J. Am. Chem. Soc.*, 2014, **136**, 5385–5399.

18 G. M. Pavan, Modelling the interaction between dendrimers and nucleic acids: a molecular perspective through hierarchical scales, *Chem. Med. Chem.*, 2014, **9**, 2623–2631.

19 M. Garzoni, K. Okuro, N. Ishii, T. Aida and G. M. Pavan, Structure and shape effects of molecular glue on supramolecular tubulin assemblies, *ACS Nano*, 2014, **8**, 904–914.

20 A. A. Skjevik, B. D. Madej, R. C. Walker and K. Teigen, LIPID11: a modular framework for lipid simulations using amber, *J. Phys. Chem. B*, 2012, **116**, 11124–11136.

21 S. Jo, J. B. Lim, J. B. Klauda and W. Im, CHARMM-GUI Membrane Builder for mixed bilayers and its application to yeast membranes, *Biophys. J.*, 2009, **97**, 50–58.

22 E. L. Wu, X. Cheng, S. Jo, H. Rui, K. C. Song, E. M. Dávila-Contreras, Y. F. Qi, J. M. Lee, V. Monje-Galvan, R. M. Venable, J. B. Klauda and W. Im, CHARMM-GUI Membrane Builder toward realistic biological membrane simulations, *J. Comput. Chem.*, 2014, **35**, 1997–2004.

23 N. Kucerca, M. P. Nieh and J. Katsaras, Fluid phase lipid areas and bilayer thicknesses of commonly used phosphatidylcholines as a function of temperature, *J. Biochim. Biophys. Acta Biomembr.*, 2011, **1808**, 2761–2771.

24 J. Wang, R. M. Wolf, J. W. Caldwell, P. A. Kollman and D. A. Case, Development and testing of a general amber force field, *J. Comput. Chem.*, 2004, **25**, 1157–1174.

25 W. L. Jorgensen, J. Chandrasekhar, J. D. Madura, R. W. Impey and M. L. Klein, Comparison of simple potential functions for simulating liquid water, *J. Chem. Phys.*, 1983, **79**, 926–935.

26 B. Klajnert, J. Janiszewska, Z. Urbanczyk-Lipkowska, M. Bryszewska and R. M. Epand, DSC studies on interactions between low molecular mass peptide dendrimers and model lipid membranes, *Int. J. Pharm.*, 2006, **327**, 145–152.

27 D. G. Mullen, A. M. Desai, J. N. Waddell, X. M. Cheng, C. V. Kelly, D. Q. McNerny, I. J. Majoros, J. R. Baker Jr., L. M. Sander, B. G. Orr and M. M. Banaszak Holl, The implications of stochastic synthesis for the conjugation of functional groups to nanoparticles, *Bioconjug. Chem.*, 2008, **19**, 1748–1752.

28 G. Franc, S. Mazères, C. O. Turrin, L. Vendier, C. Duhayon, A. M. Caminade and J. P. Majoral, Synthesis and properties of dendrimers possessing the same fluorophore(s) located either peripherally or off-center, *J. Org. Chem.*, 2007, **72**, 8707–8715.

29 A. M. Caminade, R. Laurent, C. O. Turrin, C. Rebout, B. Delavaux-Nicot, A. Ouali A, M. Zablocka and J. P. Majoral, Phosphorus dendrimers as viewed by 31P NMR spectroscopy; synthesis and characterization, *C. R. Chim.*, 2010, **13**, 1006–1027.

30 D. Chandler, Introduction to Modern Statistical Mechanics, 3rd ed.; Oxford University Press: New York, NY, 1987.

31 Y. Zhang, M. Yang, J. H. Park, J. Singelyn, H. Ma, M. J. Sailor, E. Ruoslahti, M. Ozkan and C. Ozkan, A surface-charge study on cellular-uptake behavior of F3-peptide-conjugated iron oxide nanoparticles, *Small*, 2009, **5**, 1990–1996.

32 K. Gardikis, S. Hatziantoniou, K. Viras, M. Wagner and C. A. Demetzos, DSC and Raman spectroscopy study on the effect of PAMAM dendrimer on DPPC model lipid membranes, *Int. J. Pharm.*, 2006, **318**, 118–123.

33 F. Ginhoux and S. Jung, Monocytes and macrophages: developmental pathways and tissue homeostasis, *Nat. Rev. Immunol.*, 2014, **14**, 392–404.

34 L. L. Shafer, J. A. McNulty and M. R. Young, Brain activation of monocyte lineage cells: brain-derived soluble factors differentially regulate BV2 microglia and peripheral macrophage immune functions, *Neuroimmunomodulation*, 2002, **10**, 283–294.

35 F. O. Martinez, S. Gordon, M. Locati and A. Mantovani, Transcriptional profiling of the human monocyte-to-macrophage differentiation and polarization: new molecules and patterns of gene expression, *J. Immunol.*, 2006, **177**, 7303–7311.

36 C. Schebesch, V. Kodelja, C. Muller, N. Hakij, S. Bisson, C. E. Orfanos and S. Goerdt, Alternatively activated macrophages actively inhibit proliferation of peripheral blood lymphocytes and CD4+ T cells in vitro, *Immunology*, 1997, **92**, 478–486.

37 Y. Cheng and W. H. Prusoff, Relationship between the inhibition constant (K1) and the concentration of inhibitor which causes 50 per cent inhibition (I50) of an enzymatic reaction. *Biochem. Pharmacol.*, 1973, **22**, 3099–3108.

38 M. Hayder, S. Fruchon, J. J. Fournié, M. Poupot and R. Poupot, Anti-inflammatory properties of dendrimers per se, *ScientificWorldJournal*, 2011, **11**, 1367–1382.

39 I. Teo, S. M. Toms, B. Marteyn, T. S. Barata, P. Simpson, K. A. Johnston, P. Schnupf, A. Puhar, T. Bell, C. Tang, M. Zloh, S. Matthews, P. M. Rendle, P. J. Sansonetti and S. Shaunak, Preventing acute gut wall damage in infectious diarrhoeas with glycosylated dendrimers, *EMBO Mol. Med.*, 2012, **4**, 66–81.

40 E. Blattes, A. Vercellone, H. Eutamène, C. O. Turrin, V. Théodorou, J. P. Majoral, A. M. Caminade, J. Prandi, J. Nigou and G. Puzo, Mannodendrimers prevent acute lung inflammation by inhibiting neutrophil recruitment, *Proc. Natl. Acad. Sci. USA*, 2013, **110**, 8795–8800.

41 Y. Tang, Y. Han, L. Liu, W. Shen, H. Zhang, Y. Wang, X. Cui, Y. Wang, G. Liu and R. Qi, Protective Effects and Mechanisms of G5 PAMAM Dendrimers against Acute Pancreatitis Induced by Caerulein in Mice, *Biomacromolecules*, 2015, **16**, 174–182.

42 S. M. Rele, W. Cui, L. Wang, S. Hou, G. Barr-Zarse, D. Tatton, Y. Gnanou, J. D. Esko and E. L. Chaikof, Dendrimer-like PEO glycopolymers exhibit anti-inflammatory properties, *J. Am. Chem. Soc.*, 2005, **127**, 10132–10133.

43 A. S. Chauhan, P. V. Diwan, N. K. Jain, and D. A. Tomalia. Unexpected in vivo anti-inflammatory activity observed for simple, surface functionalized poly(amidoamine) dendrimers. *Biomacromolecules*, 2009, **10**, 1195–1202.